Biochimica et Biophysica Acta 1818 (2012) 730–737

Contents lists available at SciVerse ScienceDirect

Biochimica et Biophysica Acta

journal homepage: www.elsevier.com/locate/bbamem

# Thapsigargin decreases the $Na^+$- $Ca^{2+}$ exchanger mediated $Ca^{2+}$ entry in pig coronary artery smooth muscle

Gauri Akolkar [b], Jyoti Pande [a], Sue E. Samson [a], Ashok K. Grover [a,b,*]

[a] Department of Medicine, HSC 4N41 McMaster University, Canada
[b] Department of Biology, HSC 4N41 McMaster University, 1280 Main Street West, Hamilton, ON, Canada L8S 4K1

ARTICLE INFO

*Article history:*
Received 28 July 2011
Received in revised form 28 November 2011
Accepted 30 November 2011
Available online 9 December 2011

*Keywords:*
NCX
SERCA
Immunofluorescence
Confocal microscopy
Linkage
SOCE

ABSTRACT

$Na^+$- $Ca^{2+}$ exchanger (NCX) has been proposed to play a role in refilling the sarco/endoplasmic reticulum (SER) $Ca^{2+}$ pool along with the SER $Ca^{2+}$ pump (SERCA). Here, SERCA inhibitor thapsigargin was used to determine the effects of SER $Ca^{2+}$ depletion on NCX–SERCA interactions in smooth muscle cells cultured from pig coronary artery. The cells were $Na^+$-loaded and then placed in either a $Na^+$-containing or in a $Na^+$-substituted solution. Subsequently, the difference in $Ca^{2+}$ entry between the two groups was examined and defined as the NCX mediated $Ca^{2+}$ entry. The NCX mediated $Ca^{2+}$ entry in the smooth muscle cells was monitored using two methods: $Ca^{2+}$sensitive fluorescence dye Fluo-4 and radioactive $Ca^{2+}$. $Ca^{2+}$-entry was greater in the $Na^+$-substituted cells than in the $Na^+$-containing cells when measured by either method. This difference was established to be NCX-mediated as it was sensitive to the NCX inhibitors. Thapsigargin diminished the NCX mediated $Ca^{2+}$ entry as determined by either method. Immunofluorescence confocal microscopy was used to determine the co-localization of NCX1 and subsarcolemmal SERCA2 in the cells incubated in the $Na^+$-substituted solution with or without thapsigargin. SER $Ca^{2+}$ depletion with thapsigargin increased the co-localization between NCX1 and the subsarcolemmal SERCA2. Thus, inhibition of SERCA2 leads to blockade of constant $Ca^{2+}$ entry through NCX1 and also increases proximity between NCX1 and SERCA2. This blockade of $Ca^{2+}$ entry may protect the cells against $Ca^{2+}$-overload during ischemia–reperfusion when SERCA2 is known to be damaged.



## 1. Introduction

Coronary arteries supply blood containing oxygen and nutrients to the heart. Dysfunction of coronary circulation is associated with cardiac disorders and therefore the blood flow in coronary arteries is tightly regulated [1,2]. The control of contractile force in vascular smooth muscle, which is influenced by the levels of cytosolic $Ca^{2+}$ ($[Ca^{2+}]i$), is critical to the regulation of blood flow. In the coronary artery smooth muscle, $[Ca^{2+}]i$ increases during muscle contraction and then it decreases to resting levels during muscle relaxation [3]. The increase in $[Ca^{2+}]i$ occurs by entry of extracellular $Ca^{2+}$ via $Ca^{2+}$ channels and $Na^+$-$Ca^{2+}$-exchanger (NCX, $3Na^+$: $1Ca^{2+}$) in the plasma membrane (PM), and by release of $Ca^{2+}$ sequestered in the SER [4–6]. The main pathways that lower $[Ca^{2+}]i$ are the $Ca^{2+}$ pumps residing in the SER (SERCA) and PM (PMCA), and NCX. Mitochondria may also sequester $Ca^{2+}$ and thus play a role in lowering $[Ca^{2+}]i$ [4,7–11,11–13]. SERCA sequesters $Ca^{2+}$ into the SER, whereas PMCA extrudes $Ca^{2+}$ with high affinity from the cells. NCX has a lower affinity for $Ca^{2+}$ and depending on $Na^+$ and $Ca^{2+}$ electrochemical gradients, it may expel $Ca^{2+}$ from cells (forward mode) or allow its entry (reverse mode). Another transporter, that exchanges 4 $Na^+$ for 1 $Ca^{2+}$ + 1 $K^+$, has been reported in other tissues but is not detected in the coronary artery smooth muscle. NCX are encoded by three genes: NCX1, 2 and 3 [11]. Coronary artery smooth muscle expresses NCX1 [13]. The main SERCA protein in this tissue is the splice variant b of SERCA2 [6,13].

The release of $Ca^{2+}$ from the SER $Ca^{2+}$ store is a key component in the control of $[Ca^{2+}]i$ during arterial contraction [14]. Subsequently, part of the released $Ca^{2+}$ exits the cell leading to depletion of the SER $Ca^{2+}$ store. The SER store is refilled by entry of extracellular $Ca^{2+}$ following activation of store operated $Ca^{2+}$ channels (SOCE) or reverse mode $Na^+$- $Ca^{2+}$ exchanger (NCX) [4,15–20]. Upon entry, $Ca^{2+}$ is sequestered into the SER by SERCA. Thus, SERCA in the subsarcolemmal SER and SOCE/NCX in the PM are partners in the refilling of the intracellular $Ca^{2+}$ store. Models have been proposed for the mechanism of activation of SOCE and reverse mode NCX to allow $Ca^{2+}$ entry into the cell [4,16–21]. According to one model, SER resident $Ca^{2+}$ sensor protein (STIM) undergoes rearrangement and translocation to the PM-SER junctions, where it recruits

*Abbreviations:* $[Ca^{2+}]i$, cytosolic $Ca^{2+}$; EGTA, ethyleneglycol bis (2-aminoethyl ether)-N,N,N′,N′-tetraacetic acid; NCX, $Na^+$-$Ca^{2+}$-exchanger; PBS, phosphate buffered saline; NMG, N-methylglucamine; PM, plasma membrane; SER, sarco/endoplasmic reticulum; SERCA, SR $Ca^{2+}$ pump

* Corresponding author at: Department of Medicine, HSC 4N41, McMaster University, 1280 Main Street West, Hamilton, ON Canada L8S 4K1. Tel.: +1 905 525 9140X22238.
*E-mail address:* groverak@mcmaster.ca (A.K. Grover).

0005-2736/$ – see front matter © 2011 Elsevier B.V. All rights reserved.
doi:10.1016/j.bbamem.2011.11.037

a PM residing protein (Orai) to form a channel for SOCE [15,16,22,23]. Similarly, localized elevation of intracellular $Na^+$ concentration in the PM-SER junctions may lead to activation of reverse mode NCX that is linked to SERCA mediated refilling of SER [17,20,24,25]. The close apposition of the PM and the SER also allows the preferential release of $Ca^{2+}$ from the SER towards NCX [26,27]. Based on the $[Ca^{2+}]i$ measurements in resting smooth muscle of rabbit vena cava, rapid cycling of $Ca^{2+}$ between the SER and the extracellular space was thought to be mediated by the functional linkage between NCX and SERCA [25,28]. Thus, NCX at PM-SER junctions may allow both SERCA assisted $Ca^{2+}$ refilling of the SER during cell activation and $Ca^{2+}$ extrusion during relaxation.

We have shown a functional linkage and co-distribution of NCX1 and SERCA2 in membrane fractions from smooth muscle cells cultured from pig coronary artery [27,29]. In immunofluorescence microscopic studies, we observed significant overlap in the distribution of NCX1 and SERCA2 in the smooth muscle cells [26]. To further characterize the relationship between NCX1 and SERCA2, we carried out the present study to determine the effect of SERCA inhibition on its functional and spatial co-relation with the partner protein NCX1 in smooth muscle cells from pig coronary artery. We used two methods to monitor NCX mediated $Ca^{2+}$ entry in the cells: a fluorescent $Ca^{2+}$ sensitive dye and $^{45}Ca^{2+}$ as a radioactive tracer. Inhibiting SERCA2 with thapsigargin diminished the NCX mediated $Ca^{2+}$ entry. Fluorescence microscopic co-localization of NCX1 and SERCA2 was also altered following treatment of cells with thapsigargin.

## 2. Experimental procedures

### 2.1. Cell isolation and culture

Pig coronary artery smooth muscle cells were isolated and cultured as described previously [29,30]. These cells were used on day 7 of growth in passage 4. The cells were characterized to ensure the purity and phenotype of the batch. These cells reacted positively to anti-smooth muscle α-actin which is found in the smooth muscle cells and negatively to anti-eNOS and anti-von Willebrand factor, which are found in endothelial cells. This confirms the presence of smooth muscle cells and the absence of endothelial cells in the batch of cultured cells.

### 2.2. Measurement of intracellular $Ca^{2+}$ ($[Ca^{2+}]i$)

Table 1 contains compositions of all the buffers used. The cells plated in the 96-well plates were washed twice with Makhlouf's buffer to remove the growth medium. Cells were incubated with $Ca^{2+}$ sensitive fluorescent dye Fluo-4 AM (4 μM), pluronic acid (0.02%) and probenecid (2 mM) in buffer for 45 min in the dark at room temperature (22 °C). Wells were washed twice in the Makhlouf's buffer containing probenecid to remove extracellular dye and incubated in the dark for 20 min to allow intracellular de-esterification of the dye. The cells were $Na^+$ loaded in the $Na^+$-loading buffer for 15 min in the dark. The cells were then washed twice and left in either the $Na^+$-containing MOPS buffer or $Na^+$-substituted MOPS buffer ($NMG^+$-containing MOPS buffer). The background fluorescence was recorded for 1 min before adding $CaCl_2$ (0.3 mM) to all the wells and the change in fluorescence was recorded for another 10 min at 37 °C on a fluorescence plate reader (Tecan Safire excitation 485 nm, emission 525 nm) at the Biophotonics facility at McMaster University. To normalize Fluo-4 signals, the responses from each well were calibrated by determining minimum fluorescence (Fmin) using ionophore 4Br-A23187 (6 μM) and 1 mM EGTA and maximum fluorescence (Fmax) using excess calcium (1.5 mM). Where indicated, the NCX inhibitors SEA 0400 (3 μM) and KB R7943 (10 μM) were added to cells in both $Na^+$ and $NMG^+$-containing MOPS buffer. Several compounds were prepared in DMSO and equivalent amounts of DMSO were added to the vehicle controls.

A change in $[Ca^{2+}]i$ was reported in terms of the change in fluorescence intensity of Fluo-4. The change in fluorescence was calculated for each well using the respective Fmin and Fmax obtained for that well. The percent increase in fluorescence intensity was calculated as $\Delta F = 100 * (F - F\,min)/(F\,max - F\,min)$. Slopes were calculated from the data in the first 5 min after the addition of 0.3 mM $CaCl_2$. Results from 4 different experiments were pooled and values were presented as a mean ± SEM of the specific number of replicates.

**Table 1**
Buffer compositions.

| | PBS | Makhlouf's buffer | $Na^+$-loading buffer | $Na^+$-containing MOPS buffer | $Na^+$-substituted MOPS buffer |
|---|---|---|---|---|---|
| NaCl | 137 | 115 | 140 | 140 | |
| $NMG^+$ | | | | | 140 |
| KCl | 2.7 | 5.8 | | | |
| $KH_2PO_4$ | 1.5 | 2.2 | | | |
| $NaH_2PO_4$ | 8 | | | | |
| $MgCl_2$ | 1 | 0.6 | 2 | 2 | 2 |
| Glucose | 10 | 12 | | | |
| $CaCl_2$ | 2 | 1 | | | |
| EGTA | | | 0.1 | 0.1 | 0.1 |
| HEPES-$Na^+$ | | 25 | | | |
| Nitrendipine | | | 0.01 | 0.01 | 0.01 |
| MOPS-tris | | | 20 | 20 | 20 |
| Ouabain | | | 1 | | |
| Nystatin | | | 0.025 | | |

All concentrations are in mM. The pH of all the solutions was adjusted to 7.4.

### 2.3. $^{45}Ca^{2+}$-uptake measurement

NCX mediated $^{45}Ca^{2+}$ influx was examined as described previously [29]. The cells were cultured in 60 mm Petri dishes, $Na^+$-loaded and then placed in a solution containing 50 μM $CaCl_2$ with trace amounts of $^{45}Ca^{2+}$in the $Na^+$- or $NMG^+$-containing MOPS buffer with 0 or 1 μM thapsigargin. After 5 min of gentle shaking, the cells were washed and examined for the amount of radioactivity and protein in the plate. Details of the protocol and compositions of the solutions have been described previously [29].

### 2.4. Immunofluorescence experiments

Immunofluorescence experiments were carried out on cells cultured from pig coronary artery. Each experiment was carried out over a period of two days and involved cell fixation, permeabilization, overnight incubation with primary antibodies, washing and incubation with fluorescence labeled secondary antibodies.

### 2.5. Cell fixation and permeabilization

Cells were cultured as above but grown in 35 mm tissue culture dishes each with a hole drilled through the bottom and a coverslip glued over the hole. Cells were washed three times with phosphate buffered saline (PBS) and then $Na^+$ loaded in $Na^+$ loading buffer for 15 min. The cells were then incubated for 5 min in the $NMG^+$-containing MOPS buffer with or without 3 μM thapsigargin. $CaCl_2$ (0.3 mM) was then added and the cells were incubated for another 5 min at 37 °C. The buffer was removed and the cells were fixed with 2% paraformaldehyde in PBS for 10 min [31]. Following the fixation, the cells were incubated with 0.1 M glycine in PBS to quench the effects of paraformaldehyde. Cells were washed with PBS for 10 min and then dehydrated using ice cold methanol for 15 min at −20 °C. Later, the cells were rehydrated by washing three times with PBS for 5 min. All of the non specific sites were blocked by adding 10% goat serum in PBS for 1 h at 22–24 °C.

### 2.6. Labeling with antibodies

After fixing with paraformaldehyde and blocking non specific sites, cells were incubated overnight with primary antibodies pi11-13 for NCX1 and IID8 for SERCA2 together at 4 °C (see Table 2 for antibodies). The antibodies were diluted in PBS containing 10% goat serum. Incubation without any primary antibody served as a negative control. The next day, the cells were washed twice with PBS-tween-20 (0.5%) to remove the unbound primary antibodies. The cells were fixed again with 2% paraformaldehyde for 10 min and then washed with 0.1 M glycine in PBS. Next, the cells were washed with PBS-tween 20 every 10 min for 40 min followed by incubation with the appropriate Alexa conjugated secondary antibodies. The cells were incubated for 45 min in the dark at room temperature (22 °C) with secondary antibodies goat anti-rabbit Alexa 568 and goat anti-mouse Alexa 488 against NCX1 and SERCA 2 respectively. Following the incubation, the cells were washed in the dark every 10 min for 1 h with PBS-Tween 20 to remove the unbound secondary antibodies. Finally 25 μl of Vectashield mounting medium was added to the coverslip as a mounting/anti-fade reagent for prolonged storage of samples and to prevent photobleaching.

### 2.7. Fluorescence microscopy

The cells were viewed under a confocal microscope (*Leica DMI 6000 B* SP5) using a glycerol immersion objective lens 63x 1.3NA DIC glyc HCX Pl-Apo at the Biophotonics facility at McMaster University. Fluorescent images were obtained from the top to the bottom of a cell with the z step of 0.25 μm. These images were obtained using sequential scanning with excitation wavelengths, 488 nm (Argon laser) with a 510–545 nm emission filter and 561 nm (HeNe laser) with a 600–645 nm emission filter. Image sizes were 1024×1024 pixels with 0.141 μm per pixel. These image stacks were further analyzed for co-localization as described in data analysis section.

### 2.8. Co-localization analysis

The image stacks obtained on the confocal microscope were analyzed using the program Image J (http://rsbweb.nih.gov/ij/, NIH, USA). Each image stack was opened by splitting into its two component excitation channels, 561 and 488 nm. Background was subtracted from the region of interest in each channel. Slices within an image stack were examined for the NCX1 signal and four slices with the brightest NCX1 signal from the middle of the stack were selected along with the corresponding images obtained in the SERCA2 channel. The two sets of images were interleaved in a stack. Since NCX1 is localized in the PM, small areas near the PM were selected and cropped from a selected stack. Each area of interest was rotated in such a way that PM was parallel to X-axis. From this selected and rotated area, a thin area of 10–15 μm length (parallel to the X axis) and 1–1.5 μm high (along the Y axis from the PM to the interior of cell) was selected as a region of interest and was cropped further. From each cell 20 to 30 such areas were obtained. For each cropped area the stack was then de-interleaved into the sub-stacks for each channel. The two sub-stacks from each area were further analyzed for co-localization using "Just another Co-localization Plugin (JACoP)" [32]. Manders' coefficient between two proteins, NCX1 and SERCA, were calculated as the split coefficient of M1 (fraction of NCX1 overlapping with SERCA) and M2 (fraction of SERCA overlapping with NCX1) [33]. Pearson's coefficients before and after Costes' randomization of the SERCA2 images were also analyzed [34,35]. The values obtained from different regions of the cells from five different days of experiment were pooled and presented as a mean ± SEM of the specific number of images. Appendix 1 presents the basis of the analysis conducted.

**Table 2**
Antibodies used.

| Antibody | Species | Dilution | Source |
|---|---|---|---|
| NCX – pi11-13 | Rabbit | 20× | Swant |
| SERCA – IID8 | Mouse | 20× | Affinity bioreagents |
| Anti-rabbit IgG Alexa 568 (highly cross-absorbed) | Goat | 600× | Invitrogen |
| Anti-mouse IgG Alexa 488(highly cross-absorbed) | Goat | 600× | Invitrogen |

### 2.9. Statistical analysis

Statistical analysis was performed using Instat software (San Diego, USA). An unpaired *t*-test was used for the analysis of means of two groups and an ANOVA test was used for three or more. This was followed by a Tukey-Kramer multiple comparison to test the null hypothesis. The program "Analyze a contingency table for larger contingency tables" in the Instat software package was used to determine the values of chi square for frequency distribution studies. In all instances, p-values $<0.05$ were considered significant to negate the null hypothesis.

## 3. Results

We studied the effect of the SERCA inhibitor thapsigargin on the reverse mode NCX activity and the spatial co-relation of NCX and SERCA in the smooth muscle cells from pig coronary artery.

### 3.1. $[Ca^{2+}]i$ measurements

The change in $[Ca^{2+}]i$ in the cells was monitored using the $Ca^{2+}$ sensitive fluorescent dye Fluo- 4. Cells plated in 96-well plates were loaded with Fluo-4 AM and $Na^+$ in a $Ca^{2+}$ free buffer as described in the Experimental Methods. Background fluorescence was measured in $Na^+$ loaded cells placed in $Na^+$ or $NMG^+$-containing solution. $CaCl_2$ was added to the wells and fluorescence intensity recording continued. The intensity increased at a faster rate in the cells placed in the $NMG^+$ containing solution than those in the $Na^+$ containing solution (Fig. 1A). The difference in the rate of change of fluorescence intensity in cells placed in $Na^+$ containing and $Na^+$ free solution was attributed to the NCX mediated $Ca^{2+}$ entry in cells. This entry was linear over the first 5 min and hence the difference in the rate of change of fluorescence during this time period was monitored in all the subsequent experiments (Fig. 1B). The validity of attribution to NCX1 was tested using the inhibitors KB R7943 and SEA 0400 (Fig. 1C). At high concentrations, these NCX1 inhibitors may also inhibit L-type voltage operated $Ca^{2+}$ channels [36]. Therefore, nitrendipine (10 μM), which can specifically block these $Ca^{2+}$ channels at nanomolar concentrations, was included in $Na^+$-containing and $NMG^+$-containing buffers while NCX1 mediated $Ca^{2+}$ entry in the cells was monitored [37]. In a previous study, we ruled out any role of $Na^+$- $H^+$ exchanger to account for the NCX1 activity measured under these experimental conditions [29]. When added to the cells in $NMG^+$-containing solution, both the inhibitors decreased the rate of increase in the fluorescence intensity to a level similar to that observed in the $Na^+$-containing solution [38,39]. This established the difference in the rate of change in intensity in the two solutions to be due to NCX1.

The effect of SERCA inhibitors thapsigargin and cyclopiazonic acid was first tested in control cells placed only in the Makhlouf's buffer (contains 1 mM $CaCl_2$) and not subjected to any of the other treatments. Both the agents caused a transient increase in $[Ca^{2+}]i$ (Fig. 2). When thapsigargin was added, $[Ca^{2+}]i$ returned to near basal levels in less than 5 min. Thus, it was established that the cells respond to the SERCA inhibitors and that this response was a

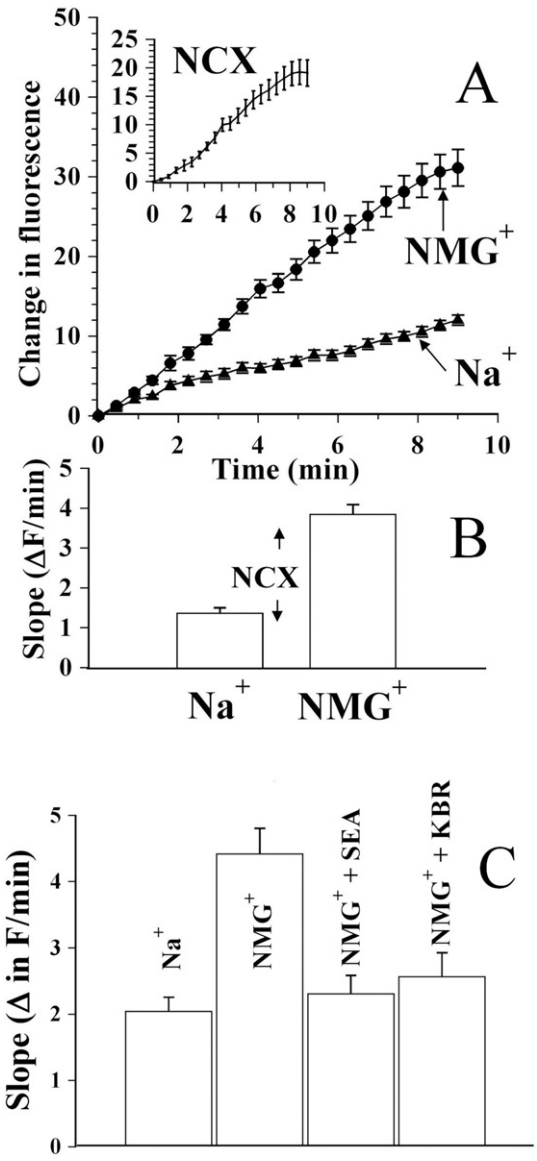


**Fig. 1.** NCX mediated increase in $[Ca^{2+}]i$ measured as a change in the Fluo-4 fluorescence intensity. A. Time Course. Increase in fluorescence intensity in buffers containing $Na^+$ or $NMG^+$. The inset shows the difference between the fluorescence intensity obtained for $NMG^+$ and $Na^+$, and represents the increase in fluorescence intensity due to NCX mediated increase in $[Ca^{2+}]i$. The results were pooled from 8 different experiments in a total number of 109 wells for $Na^+$ and 118 for $NMG^+$. B. Slope in change of fluorescence (ΔF) in first 5 min from tracings in A. C. Pharmacological characterization of NCX mediated increase in $[Ca^{2+}]i$. The mean ± SEM and number of replicates for the various groups were $Na^+$: 2.04 ± 0.21 (43), $NMG^+$: 4.42 ± 0.39 (42), SEA 0400 + $NMG^+$ : 2.31 ± 0.28 (30), KB R7943 plus $NMG^+$ : 2.57 ± 0.36 (28). One way Anova followed by a multiple comparison with the Tukey-Kramer test showed that the $NMG^+$ group value was larger than the following groups: SEA 0400 + $NMG^+$ ($Q = 6.542$, $p < 0.001$), KB R7943 plus $NMG^+$ ($Q = 5.623$, $p < 0.001$) and $Na^+$ ($Q = 8.125$, $p < 0.001$). The groups $NMG^+$ plus SEA0400 ($Q = 0.8359$, $p > 0.05$) and $NMG^+$ plus KB R7943 ($Q = 1.609$, $p > 0.05$) were not significantly different from the $Na^+$ group.

transient one. The return of the $[Ca^{2+}]i$ transient to near basal levels was slightly faster in cells treated with thapsigargin (5 min), which was used in subsequent experiments to deplete the SER $Ca^{2+}$ pool.

To determine the effect of thapsigargin on the NCX1 mediated increase in $[Ca^{2+}]i$, the cells were $Na^+$ loaded in a $Ca^{2+}$ free buffer and then transferred into a solution containing $Na^+$ or into a solution in which $Na^+$ had been substituted with $NMG^+$, and then thapsigargin was added to some wells and other wells were used for vehicle

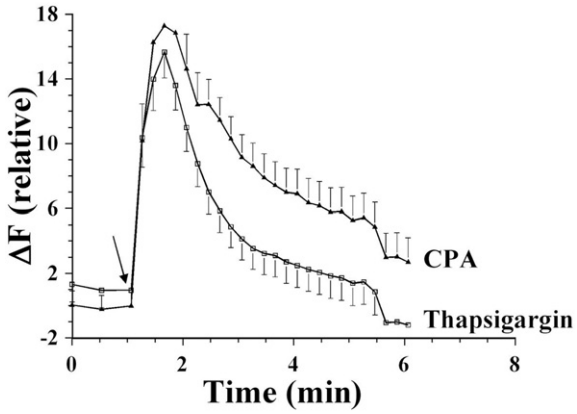


**Fig. 2.** SERCA inhibitors transiently increased $[Ca^{2+}]i$ in control cells without any treatment. The fluorescence was monitored and the inhibitors, or the vehicle control, were added as shown by the arrow and the monitoring was continued. The basal level of fluorescence was subtracted from each well. The data are pooled from experiments on several days and the total number of wells was 56 for thapsigargin, 54 for CPA and 34 for the vehicle control. The mean values for the vehicle control were subtracted from each time point before graphing the data. The values shown are mean ± SEM.

control. After determining the background fluorescence, extracellular $CaCl_2$ was added to all the cells and the rate of change in fluorescence was recorded for another 5 min (Fig. 3). Thapsigargin inhibited the rate of change of fluorescence in cells in $NMG^+$-containing solution (Fig. 3). In contrast, there was no difference in the rate of change of fluorescence in cells in the $Na^+$-containing solution in the presence or absence of thapsigargin. Thus, thapsigargin diminished the NCX1 mediated increase in $[Ca^{2+}]i$ without affecting the non-NCX1 mediated $Ca^{2+}$ entry in the smooth muscle cells.

### 3.2. $^{45}Ca^{2+}$ uptake

The NCX1-mediated $^{45}Ca^{2+}$ uptake was compared in $Na^+$-loaded cells as a difference between the uptake in the $Na^+$-containing and $NMG^+$-containing solutions. Thapsigargin diminished the NCX1-mediated $^{45}Ca^{2+}$ entry (Fig. 4).

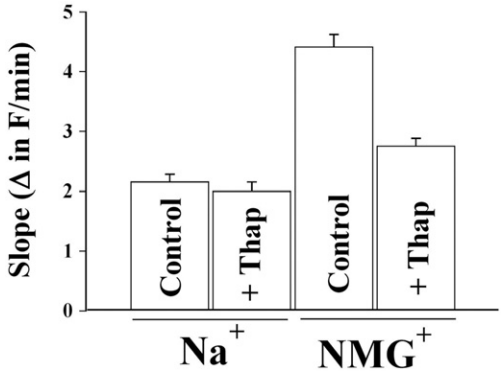


**Fig. 3.** Effect of thapsigargin on NCX mediated increase in $[Ca^{2+}]i$. The mean ± SEM and number of replicates for the various groups were $Na^+$: 2.15 ± 0.133 (64), thapsigargin plus $Na^+$:2.0 ± 0.15 (54), $NMG^+$: 4.41 ± 0.21 (55) and thapsigargin plus $NMG^+$: 2.75 ± 0.13 (57). One way Anova followed by a multiple comparison with Tukey-Kramer test showed that the $NMG^+$ group had a larger value than the groups thapsigargin plus $NMG^+$ ($Q = 10.366$, $p < 0.001$) or $Na^+$ ($Q = 14.517$, $p < 0.001$). However the inhibition was not complete since the value for the group thapsigargin plus $NMG^+$ was also slightly larger than the group $Na^+$ ($Q = 3.897$, $p < 0.05$). Also thapsigargin did not affect the values in the $Na^+$ group ($Q = 0.9587$, $p > 0.05$).

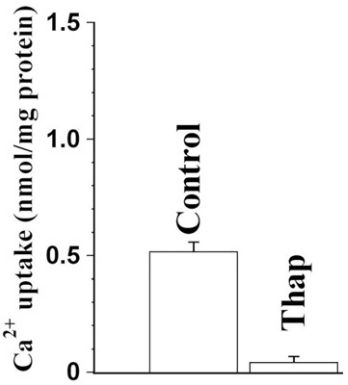


**Fig. 4.** Effect of thapsigargin on NCX1 mediated $^{45}Ca^{2+}$ entry for 5 min. The mean value of the NCX1 mediated uptake from 5 to 6 plates on a single day was taken as one replicate. The values for mean ± SEM of NCX1 mediated uptake and number of replicates for the various groups were control: 0.52 ± 0.04 (15) and thapsigargin: 0.04 ± 0.03 (8). The two values differed significantly ($p<0.0001$).

### 3.3. Co-localization of NCX1 and SERCA2

Immunofluorescence confocal microscopy using antibodies against NCX1 and SERCA2 were used to examine the co-localization of the two proteins. The basis of this analysis is presented in Appendix 1. The protocol was first optimized for various parameters: cell fixation, cell permeabilization, antibody staining, microscopy and image acquisition. Fig. 5 shows a representative image for the NCX1 detection (Fig. 5A), SERCA detection (5B) and the overlap in the distribution of the two proteins shown in white (Fig. 5C). Since the detection of the primary antibodies was based on fluorescent secondary antibodies, control images without the primary antibodies were also examined (Fig. 5D and E). These images did not show any significant staining compared to the images obtained using both primary and secondary antibodies.

Stacks containing interleaved images of cells stained with anti-NCX1 (561 nm) and anti-SERCA2 (488 nm) were next used to examine whether the two proteins are co-distributed in the subsarcolemmal domains of the cells. For each cell, slices showing the brightest stain for NCX1 were chosen and subsarcolemmal domains were numbered (Fig. 6). Each numbered domain was then cropped and rotated such that the PM was horizontal. The sections were then cropped (10–15 × 1–1.5 μm), de-interleaved and analyzed for co-distribution of the two proteins. Four types of parameters were determined. Co-distribution of the two proteins was determined as Pearson's coefficient ($R_{original}$). For each substack, the SERCA2 images were randomized and the $R_{random}$ value was determined again. The fraction of NCX1 that co-distributed with SERCA2 was determined as the Manders' coefficient M1 and similarly the fraction of SERCA2 that co-distributed with NCX was determined as M2.

The cells were $Na^+$-loaded and placed in the $NMG^+$-containing solution with or without thapsigargin and then analyzed as shown in Fig. 6. In five experiments, a total of 514 areas were analyzed for 68 cells without thapsigargin treatment and 617 areas from 71 cells with thapsigargin treatment. The values of $R_{original}$, $R_{random}$ (obtained by randomization of the SERCA2 images), M1 and M2 are shown in Table 3. The significant probability of co-localization of NCX1 and SERCA2 as indicated by the observed values of R was not due to random chance because $R_{random}$ values were significantly lower than the $R_{original}$ values. NCX1 is known to be in the plasma membrane and not in the deep cytoplasmic regions of the cells. Therefore, the data were also analyzed using cytoplasmic regions from the same images (Fig. 6, Appendix 1). The values for M1, M2 and $R_{original}$ that were obtained from the subsarcolemmal regions were significantly larger

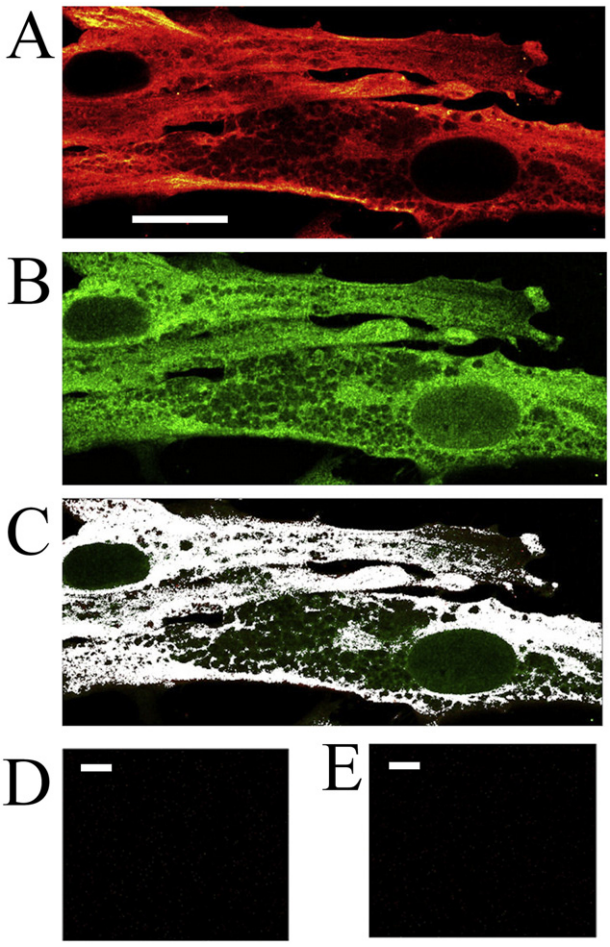


**Fig. 5.** Dual excitation immunofluorescence confocal microscopy images from middle stacks. A. Cells labeled with anti-NCX1and secondary antibody goat anti-rabbit Alexa 568. B. Same cells labeled with anti SERCA2 and secondary antibody goat anti-mouse Alexa 488. C. Overlap of NCX1 and SERCA2 images. Overlap is shown in white. D and E are negative control images with only the secondary antibodies, goat anti-rabbit Alexa 568 and goat anti-mouse Alexa 488, respectively. Length of the bar = 20 μm.

than those from the deep cytoplasmic regions. Thus, the co-localization of NCX1 and SERCA2 in the subsarcolemmal regions was confirmed with the comparison using images from two types of negative controls: randomization and deep cytoplasmic region analysis (Appendix 1).

Thapsigargin treatment showed a significant increase in the $R_{original}$ values as compared to the vehicle control cells. The values of M1 were greater than those of M2 for both thapsigargin treated and untreated cells. Thapsigargin increased the M1 and M2 values as compared to vehicle control cells, with increase in M1 being larger as compared to M2. The data were also analyzed for the frequency distribution of the R, M1 and M2 values (Fig. 7). Thapsigargin treatment shifted the frequency distributions to higher values for $R_{original}$ (Chi square = 47.631, $p<0.0001$), M1 (Chi square = 54.699, $p<0.0001$), and M2 (Chi square = 45.250, $p<0.0001$). Thus the mean value and frequency distribution analyses showed that thapsigargin treatment increased the cross co-localization between NCX1 and SERCA2, increased the fraction of NCX1 co-distributed with SERCA2 and to a smaller extent increased the SERCA2 co-distributed with NCX1. Appendix 1 shows that the effects of thapsigargin were observed only in the subsarcolemmal region images and lost upon randomization. They were also absent when cytoplasmic region images were analyzed.

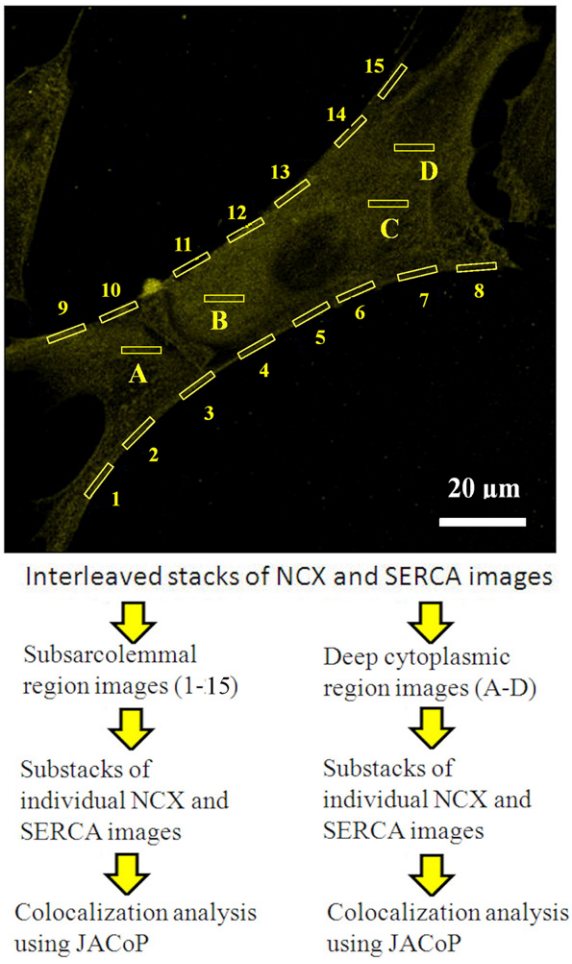


**Fig. 6.** Steps involved in co-localization analysis of NCX1 and SERCA2. Confocal images were obtained by dual excitation immunofluorescence for anti-NCX and anti-SERCA antibodies. From the middle of the stack 4 contiguous slices with the brightest staining for NCX were selected and interleaved with the corresponding images for SERCA2. Several regions of 10–15 × 1–1.5 µm in the subsarcolemmal domain (numbered 1–15 in the figure) and cytoplasmic domains (labeled A,B,C,D) were chosen from stacks for further analysis. For analysis of each region, the stack was rotated such that the long axis of the image was horizontal. The stack of images was then cropped to obtain the desired region and de-interleaved to obtain substacks for NCX1 and SERCA2. The substacks were analyzed for co-localization using JACoP.

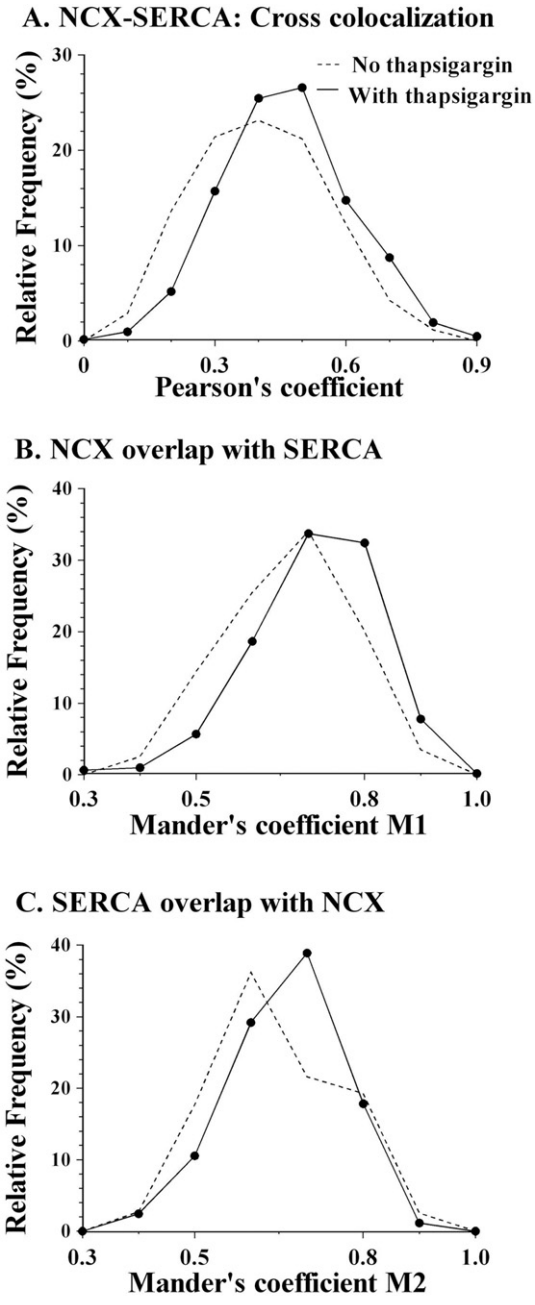


**Fig. 7.** Effect of thapsigargin on overlap between NCX1 and SERCA2 in the subsarcolemmal domains. A. NCX1-SERCA2 cross co-localization. B. Fraction of NCX1 overlapping with SERCA2. C. Fraction of SERCA2 overlapping with NCX1. Image stacks from 68 cells placed in $NMG^+$ alone were analyzed as a total of 514 regions. For the $NMG^+$ plus thapsigargin experiment 71 cells were analyzed as 617 regions. From each region Pearson's coefficient, M1 (NCX1 overlap with SERCA2) and M2 (SERCA2 overlap with NCX1) were determined. Frequency distribution for each parameter was expressed as relative frequency distribution and plotted.

## 4. Discussion

NCX1 mediated $Ca^{2+}$ entry in the cells was observed both as an increase in the fluorescence intensity of $Ca^{2+}$ sensitive dye and as the uptake of radioactive $Ca^{2+}$. This NCX1 mediated $[Ca^{2+}]i$ increase observed with both the methods was diminished following inhibition of the SERCA2 pump with thapsigargin. $Ca^{2+}$ depletion from the SER with thapsigargin also increased the co-localization of NCX1 and SERCA2 in the subsarcolemmal domain. The discussion focuses on the experimental methodology used in the present study, comparison of the key observations with literature and the significance of these findings.

**Table 3**
The effect of thapsigargin treatment on various overlap parameters (Mander's and Pearson's coefficient using Costes randomization) in $Na^+$-loaded cells in $NMG^+$ solution.

| | $NMG^+$ | $NMG^+$-Thapsigargin | t-value | P value |
|---|---|---|---|---|
| M1 | 0.617 ± 0.005 | 0.663 ± 0.004 | 7.254 | <0.001 |
| M2 | 0.595 ± 0.005 | 0.616 ± 0.004 | 3.402 | 0.001 |
| $R_{original}$ | 0.356 ± 0.007 | 0.415 ± 0.006 | 6.704 | <0.001 |
| $R_{random}$ | 0.088 ± 0.004 | 0.087 ± 0.004 | 0.150 | 0.881 |

The values are mean ± SEM of 514 regions for $NMG^+$ and 617 regions for $NMG^+$-Thapsigargin.

NCX1 mediated $Ca^{2+}$ entry may be examined using electrophysiological techniques, $Ca^{2+}$ sensitive fluorescent probes, $^{45}Ca^{2+}$ uptake in $Na^+$-loaded cells or functional studies. Each method has its own advantages and pitfalls. In this study, we used a $Ca^{2+}$ sensitive dye and the radioactive isotope $^{45}Ca^{2+}$ to examine the NCX1 mediated changes in $[Ca^{2+}]i$ in the smooth muscle cells. The results obtained with the two methods were consistent with each other and with

the pharmacological characterization using the NCX inhibitors KB R7943 and SEA 0400.

We used thapsigargin to study the effect of SERCA2 inhibition on its functional linkage and spatial correlation with NCX1. Thapsigargin has been used extensively to cause depletion of the SER $Ca^{2+}$ pool. We observed an inhibition of the NCX1 mediated $Ca^{2+}$ entry in the smooth muscle cells in the presence of thapsigargin. Thus, thapsigargin modulates the functional linkage between NCX and SERCA2.

Co-localization of NCX1 and SERCA2 in the cells was determined using immunofluorescence microscopy. We have previously validated this method using several positive and negative controls [26]. Appendix 1 also contains details of the basis of this analysis. SERCA2 inhibition by thapsigargin led to an increase in the co-distribution of NCX1 and SERCA ($R_{original}$), the fraction of NCX co-distributed with SERCA2 (M1) and to a smaller extent, the fraction of SERCA2 co-distributed with NCX1 (M2). A smaller increase in M2 as compared to M1 is expected as only the peripheral component of total SER has been shown to move closer to PM to form nanodomains. The area analyzed for our co-localization study was 1–1.5 μm deep into the cell and a much higher SERCA content is found in the extensive SER in the cell interior. These results suggest that the depletion of intracellular $Ca^{2+}$ stores by thapsigargin increases the proximity between NCX1 and subsarcolemmal SERCA2. In studies on other cell types, it has been shown that depleting $Ca^{2+}$ from the SER leads to an increase in proximity between the sarcolemmal protein Orai and the SER protein STIM to form the store operated $Ca^{2+}$ channels [15,16,21–23]. In the subsarcolemmal SER, SERCA2 is also co-localized with STIM [40]. Thapsigargin has been shown to increase an association between the lipid raft resident TRPC1 protein with STIM [19]. NCX is also a lipid raft resident protein [27]. Therefore, one cannot rule out the possibility that the observed thapsigargin induced increase in the proximity between NCX1 and SERCA2 results from the spatial reorganization of other proteins in their proximity.

A functional linkage where $Ca^{2+}$ entry by reverse mode NCX refills the SER $Ca^{2+}$ pool has been suggested in various other tissues [17,20,24,25,28]. A linked transport of $Ca^{2+}$ between NCX and SERCA may result due to close apposition of the SER to the PM [26,27]. In vascular smooth muscle, a "junctional cytoplasmic space model" has been proposed. In this model, NCX and SERCA occur in a close complex within a narrow cytoplasmic space between the subsurface SER and the PM allowing for restricted $Ca^{2+}$ diffusion and a functional linkage [17,20,28]. We postulate that thapsigargin treatment leads directly or indirectly to an organellar rearrangement that further restricts diffusion between the junctional space and the cytoplasm. Although one cannot rule out the role of mitochondria in close proximity to SER, a possibility is that SERCA inhibition causes $Ca^{2+}$ to accumulate in the limited diffusional space between the PM and the superficial SER leading to a shift in the reverse potential of NCX and inhibition of NCX mediated $Ca^{2+}$ entry. This is supported by our observation that thapsigargin also leads to increased proximity between NCX and SERCA. Although the exact mechanism behind this spatial rearrangement is unclear, it is speculated that this would further tighten the junctional complexes. It is not known if there is a cause and effect relationship between the decreased NCX mediated $Ca^{2+}$ entry and the spatial rearrangement. The spatial rearrangement also raises several questions that need to be addressed. STIM family of proteins involved in SOCE also reside in SER like SERCA. Like reverse mode NCX, SOCE is also an important partner in refilling the empty SER $Ca^{2+}$ pool. It needs to be determined if the activity of SOCE is influenced by spatial co-relation of the peripheral SER and PM in the cells. Do these two $Ca^{2+}$ refilling pathways operate independently or does disruption of one affect the activity of the other? In one study, it has been suggested that NCX overexpression may enhance SOCE [41]. Also, does $Ca^{2+}$ elevation in the limited subsarcolemmal domain affect the voltage operated channels which have been suggested to enhance SER refilling [24]?

A pathophysiological implication of the reported observations is that the inhibition of SERCA blocks the constant $Ca^{2+}$ entry through NCX and prevent cellular damage due to excessive $[Ca^{2+}]i$. The increase in NCX mediated $Ca^{2+}$ entry was diminished with an inhibition of SERCA activity with thapsigargin. Peroxide, superoxide and peroxynitrite can severely damage SERCA in the pig coronary artery smooth muscle [6]. Thus, inhibition of NCX mediated $Ca^{2+}$ entry and organellar rearrangement may protect the cells from severe damage during ischemia–reperfusion when SERCA is not functional.

## Acknowledgements

This work was funded by a grant-in-aid from Heart & Stroke Foundation of Ontario. We thank Shawn Grover for writing a protocol for transferring data from text files to Excel and we acknowledge Dr. E.E. Daniel for his suggestions on the manuscript.

## Appendix 1. Supplementary data

Supplementary data to this article can be found online at doi:10.1016/j.bbamem.2011.11.037.

## References

[1] D. Merkus, D.J. Duncker, W.M. Chilian, Metabolic regulation of coronary vascular tone: role of endothelin-1, Am. J. Physiol. Heart Circ. Physiol. 283 (2002) H1915–H1921.
[2] F.T. Range, M. Schafers, T. Acil, K.P. Schafers, P. Kies, M. Paul, S. Hermann, B. Brisse, G. Breithardt, O. Schober, T. Wichter, Impaired myocardial perfusion and perfusion reserve associated with increased coronary resistance in persistent idiopathic atrial fibrillation, Eur. Heart J. 28 (2007) 2223–2230.
[3] M. Brini, E. Carafoli, Calcium pumps in health and disease, Physiol. Rev. 89 (2009) 1341–1378.
[4] D.E. Clapham, Calcium signaling, Cell 131 (2007) 1047–1058.
[5] A.K. Grover, I. Khan, Calcium pump isoforms: diversity, selectivity and plasticity. Review article, Cell Calcium 13 (1992) 9–17.
[6] C.M. Misquitta, D.P. Mack, A.K. Grover, Sarco/endoplasmic reticulum Ca2+ (SERCA)-pumps: link to heart beats and calcium waves, Cell Calcium 25 (1999) 277–290.
[7] E. Carafoli, Historical review: mitochondria and calcium: ups and downs of an unusual relationship, Trends Biochem. Sci. 28 (2003) 175–181.
[8] Y. Kirichok, G. Krapivinsky, D.E. Clapham, The mitochondrial calcium uniporter is a highly selective ion channel, Nature 427 (2004) 360–364.
[9] S.A. John, B. Ribalet, J.N. Weiss, K.D. Philipson, M. Ottolia, Ca2+−dependent structural rearrangements within Na+−Ca2+ exchanger dimers, Proc. Natl. Acad. Sci. U. S. A. 108 (2011) 1699–1704.
[10] R. Larbig, N. Torres, J.H. Bridge, J.I. Goldhaber, K.D. Philipson, Activation of reverse Na+−Ca2+ exchange by the Na+ current augments the cardiac Ca2+ transient: evidence from NCX knockout mice, J. Physiol. 588 (2010) 3267–3276.
[11] J. Lytton, Na+/Ca2+ exchangers: three mammalian gene families control Ca2+ transport, Biochem. J. 406 (2007) 365–382.
[12] P. Neco, B. Rose, N. Huynh, R. Zhang, J.H. Bridge, K.D. Philipson, J.I. Goldhaber, Sodium–calcium exchange is essential for effective triggering of calcium release in mouse heart, Biophys. J. 99 (2010) 755–764.
[13] M.M. Szewczyk, K.A. Davis, S.E. Samson, F. Simpson, P.K. Rangachari, A.K. Grover, Ca2+−pumps and Na2+−Ca2+−exchangers in coronary artery endothelium versus smooth muscle, J. Cell. Mol. Med. 11 (2007) 129–138.
[14] R. Floyd, S. Wray, Calcium transporters and signalling in smooth muscles, Cell Calcium 42 (2007) 467–476.
[15] M.D. Cahalan, STIMulating store-operated Ca(2+) entry, Nat. Cell Biol. 11 (2009) 669–677.
[16] N. Calloway, M. Vig, J.P. Kinet, D. Holowka, B. Baird, Molecular clustering of STIM1 with Orai1/CRACM1 at the plasma membrane depends dynamically on depletion of Ca2+ stores and on electrostatic interactions, Mol. Biol. Cell 20 (2009) 389–399.
[17] N. Fameli, C. van Breemen, K.H. Kuo, A quantitative model for linking Na+/Ca2+ exchanger to SERCA during refilling of the sarcoplasmic reticulum to sustain [Ca2+] oscillations in vascular smooth muscle, Cell Calcium 42 (2007) 565–575.
[18] T. Hewavitharana, X. Deng, J. Soboloff, D.L. Gill, Role of STIM and Orai proteins in the store-operated calcium signaling pathway, Cell Calcium 42 (2007) 173–182.
[19] B. Pani, H.L. Ong, X. Liu, K. Rauser, I.S. Ambudkar, B.B. Singh, Lipid rafts determine clustering of STIM1 in endoplasmic reticulum-plasma membrane junctions and regulation of store-operated Ca2+ entry (SOCE), J. Biol. Chem. 283 (2008) 17333–17340.
[20] D. Poburko, N. Fameli, K.H. Kuo, C. van Breemen, Ca2+ signaling in smooth muscle: TRPC6, NCX and LNats in nanodomains, Channels (Austin) 2 (2008) 10–12.
[21] L. Vaca, SOCIC: the store-operated calcium influx complex, Cell Calcium 47 (2010) 199–209.
[22] J.W. Putney Jr., Recent breakthroughs in the molecular mechanism of capacitative calcium entry (with thoughts on how we got here), Cell Calcium 42 (2007) 103–110.

[23] J. Soboloff, M.A. Spassova, M.A. Dziadek, D.L. Gill, Calcium signals mediated by STIM and Orai proteins—a new paradigm in inter-organelle communication, Biochim. Biophys. Acta 1763 (2006) 1161–1168.
[24] S. Hirota, L.J. Janssen, Store-refilling involves both L-type calcium channels and reverse-mode sodium–calcium exchange in airway smooth muscle, Eur. Respir. J. 30 (2007) 269–278.
[25] C.H. Lee, D. Poburko, P. Sahota, J. Sandhu, D.O. Ruehlmann, C. van Breemen, The mechanism of phenylephrine-mediated [Ca(2+)](i) oscillations underlying tonic contraction in the rabbit inferior vena cava, J. Physiol. 534 (2001) 641–650.
[26] I. Kuszczak, R. Kuner, S.E. Samson, A.K. Grover, Proximity of Na+ −Ca2+ −exchanger and sarco/endoplasmic reticulum Ca2+ pump in pig coronary artery smooth muscle: fluorescence microscopy, Mol. Cell. Biochem. 339 (2010) 293–300.
[27] I. Kuszczak, S.E. Samson, J. Pande, D.Q. Shen, A.K. Grover, Sodium-calcium exchanger and lipid rafts in pig coronary artery smooth muscle, Biochim. Biophys. Acta 1808 (2011) 589–596.
[28] C.H. Lee, D. Poburko, K.H. Kuo, C. Seow, C. van Breemen, Relationship between the sarcoplasmic reticulum and the plasma membrane, Novartis Found. Symp. 246 (2002) 26–41.
[29] K.A. Davis, S.E. Samson, K.E. Hammel, L. Kiss, F. Fulop, A.K. Grover, Functional linkage of Na+−Ca2+−exchanger to sarco/endoplasmic reticulum Ca2+ pump in coronary artery: comparison of smooth muscle and endothelial cells, J. Cell. Mol. Med. 13 (2009) 1775–1783.
[30] A.K. Grover, S.E. Samson, Peroxide resistance of ER Ca2+ pump in endothelium: implications to coronary artery function, Am. J. Physiol. 273 (1997) C1250–C1258.
[31] C.C. Ho, P.H. Huang, H.Y. Huang, Y.H. Chen, P.C. Yang, S.M. Hsu, Up-regulated caveolin-1 accentuates the metastasis capability of lung adenocarcinoma by inducing filopodia formation, Am. J. Pathol. 161 (2002) 1647–1656.
[32] S. Bolte, F.P. Cordelieres, A guided tour into subcellular colocalization analysis in light microscopy, J. Microsc. 224 (2006) 213–232.
[33] E.E.M. Manders, F.J. Verbeek, J.A. Aten, Measurement of co-localization of objects in dual-colour confocal images, J. Microsc. 169 (1993) 375–382.
[34] S.V. Costes, D. Daelemans, E.H. Cho, Z. Dobbin, G. Pavlakis, S. Lockett, Automatic and quantitative measurement of protein-protein colocalization in live cells, Biophys. J. 86 (2004) 3993–4003.
[35] K. Pearson, Mathematical contributions to the theory of evolution III. Regression, heredity and panmixia, Philos. Trans. R. Soc. Lond. B Biol. Sci. 187 (2011) 253–318.
[36] P. Birinyi, K. Acsai, T. Banyasz, A. Toth, B. Horvath, L. Virag, N. Szentandrassy, J. Magyar, A. Varro, F. Fulop, P.P. Nanasi, Effects of SEA0400 and KB-R7943 on Na+/Ca2+ exchange current and L-type Ca2+ current in canine ventricular cardiomyocytes, Naunyn Schmiedebergs Arch. Pharmacol. 372 (2005) 63–70.
[37] A.K. Grover, P.J. Oakes, Calcium channel antagonist binding and pharmacology in rat uterine smooth muscle, Life Sci. 37 (1985) 2187–2192.
[38] T. Iwamoto, Forefront of Na+/Ca2+ exchanger studies: molecular pharmacology of Na+/Ca2+ exchange inhibitors, J. Pharmacol. Sci. 96 (2004) 27–32.
[39] T. Iwamoto, S. Kita, Development and application of Na+/Ca2+ exchange inhibitors, Mol. Cell. Biochem. 259 (2004) 157–161.
[40] I.M. Manjarres, A. Rodriguez-Garcia, M.T. Alonso, J. Garcia-Sancho, The sarco/endoplasmic reticulum Ca(2+) ATPase (SERCA) is the third element in capacitative calcium entry, Cell Calcium 47 (2010) 412–418.
[41] G. Chernaya, M. Vazquez, J.P. Reeves, Sodium-calcium exchange and store-dependent calcium influx in transfected chinese hamster ovary cells expressing the bovine cardiac sodium-calcium exchanger. Acceleration of exchange activity in thapsigargin-treated cells, J. Biol. Chem. 271 (1996) 5378–5385.